Biosensors and Bioelectronics 51 (2014) 191–194

Contents lists available at ScienceDirect

Biosensors and Bioelectronics

journal homepage: www.elsevier.com/locate/bios

Short communication

Ultrasensitive electrochemical cocaine biosensor based on reversible DNA nanostructure

Qinglin Sheng, Ruixiao Liu, Sai Zhang, Jianbin Zheng *

Institute of Analytical Science, Shaanxi Provincial Key Laboratory of Electroanalytical Chemistry, Northwest University, Xi'an, Shaanxi 710069, PR China

ARTICLE INFO

Article history:
Received 4 June 2013
Received in revised form
24 July 2013
Accepted 25 July 2013
Available online 2 August 2013

Keywords:
Biosensor
DNA nanostructure
Impedance spectroscopy
Aptamer
Cocaine

ABSTRACT

We proposed an ultrasensitive electrochemical cocaine biosensor based on the three-dimensional (3D) DNA structure conversion of nanostructure from Triangular Pyramid Frustum (TPF_{DNA}) to Equilateral Triangle (ET_{DNA}). The presence of cocaine triggered the aptamer-composed DNA nanostructure change from "Close" to "Open", leading to obvious faradaic impedance changes. The unique properties with excellent stability and specific rigid structure of the 3D DNA nanostructure made the biosensing functions stable, sensitive, and regenerable. The Faradaic impedance responses were linearly related to cocaine concentration between 1.0 nM and 2.0 μM with a correlation coefficient of 0.993. The limit of detection was calculated to be 0.21 nM following IUPAC recommendations ($3S_b/b$). It is expected that the distinctive features of DNA nanostructure would make it potentially advantageous for a broad range of biosensing, bionanoelectronics, and therapeutic applications.

1. Introduction

Highly sensitive and selective biosensing based on nucleic acids is recently proved to be valuable for the quantitative detection of nucleic acids and indirect detection of other targets. Among the many exciting achievements on nucleic acid-based biosensors, aptamers have been engineered as biorecognition elements to integrate affinity and signal transducing moieties into the ultrasensitive biosensing strategies (Willner and Zayats, 2007; Liu et al., 2009; Zhou et al., 2010; Xiang et al., 2011; Yeung et al., 2010).

Despite their impressive performances, technologies based on DNA assembly on electrode surface and their recognition processes still suffer from the inherent limitations of stability and irreversibility, which commonly relies on single DNA sequence anchored on electrode by SH-group and the recognition relying on DNA hydrolysis (Carrasquilla et al., 2012; Wang et al., 2011a), or through the use of single-stranded "toeholds" to initiate strand-displacement reactions (Soloveichik et al., 2010; Yang and Lai, 2012). To solve these problems, much recent progress has been made in developing three-dimensional (3D) DNA architectures (Douglas et al., 2009; Li et al., 2009; Pei et al., 2012). The construction of artificial DNA nanostructure with nearly arbitrary 3D nanostructure has brought us a great revolution for bioelectronics and biosensors (Kang et al., 2012; Vallée-Bélisle et al., 2011; Surana et al., 2011; Wang et al., 2011b). Yan and Fan's groups have devised a new concept to achieve improved probe–target recognition properties by constructing a "pyramidal" DNA tetrahedra structure-based chip platform (Pei et al., 2010). The 3D nanostructured recognition probes anchored at Au surfaces have been proved to have mechanical rigidity and structural stability. Based on the DNA nanostructure-decorated sensing protocol, they have developed an ultrasensitive and highly selective electrochemical aptamer-based cocaine sensor (Wen et al., 2011). Because the aptamer probe-pendant tetrahedral DNA nanostructure can greatly facilitate cocaine-induced fusion of the split anticocaine aptamer, a remarkably low detection limit of 33 nM was obtained. Moreover, the tetrahedron-decorated surface is protein-resistant, making the DNA nanostructure-decorated sensing platform suit the enzyme-based amplification system and ensures high selectivity of the sensor. Jiang et al. have demonstrated a new strategy for highly sensitive electrochemical detection of cocaine by using two engineered aptamers in connection to redox-recycling signal amplification and a low nanomolar (1 nM) detection limit was achieved (Jiang et al., 2012). Bearing this concept in mind, we may expect that utilizing the superiority of 3D DNA nanostructure, the construction of novel sensitive, selective and reversible biosensors might prove effective as delivery vehicles, beyond what is possible with traditional linear or stem-loop probe structures DNA forms.

To demonstrate the general design of the 3D DNA nanostructure based biosensing platform, we first use cocaine and its aptamer as the pair of target–aptamer for a proof of concept. Scheme 1 outlines the principle for the construction of 3D DNA nanostructure and sensing process. 1.0 mM $Fe(CN)_6^{3-/4-}$ was employed as the electron indicator to monitor the "Open" and "Close" states. The initial Triangular Pyramid Frustum nanostructure (defined as TPF_{DNA}) was first hierarchically assembled from five stoichiometric equivalents DNA probes, three thiolated DNA probes (P1, P2, and P3) of 36

* Corresponding author. Tel.: +86 29 88302077; fax: +86 29 88303448.
E-mail address: zhengjb@nwu.edu.cn (J. Zheng).

0956-5663/$ - see front matter © 2013 Elsevier B.V. All rights reserved.
http://dx.doi.org/10.1016/j.bios.2013.07.053

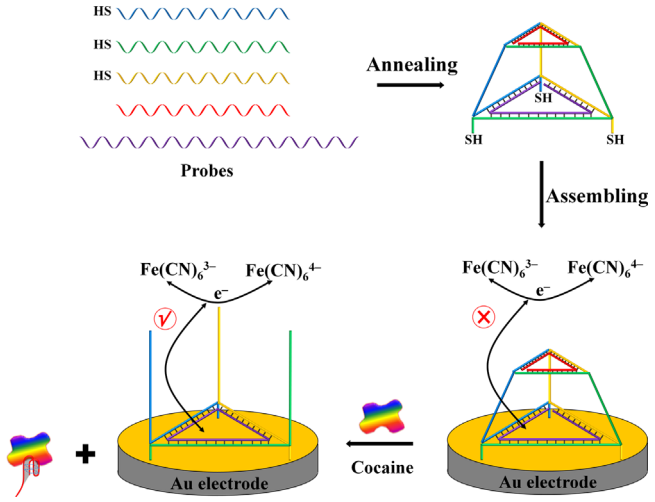

Scheme 1. Schematic illustration of the cocaine sensing based on TPF_{DNA} nanostructure assembled on Au electrode.

nucleotides (40-nt), one 55-nt DNA probe (P4) and one 39-base cocaine aptamer probe (P5). Here, the P4 sequence composed of three equal parts of 17-base fragments can specifically bind to the relative 5′-end of the three thiolated probes, and the P5 was fully complementary to the 3′-end of the 13-base fragments of thiolated P1, P2, and P3 which allows the formation of a short 13-base DNA duplex at the distal end of the probes. After incubation of an Au electrode in TPF_{DNA} solution, TPF_{DNA} assembled onto Au electrode surfaces by the three thiol groups was formed. In this state, the electron transfer of $Fe(CN)_6^{3-/4-}$ was greatly inhibited, due to the formation of the 3D TPF_{DNA} that prevents $Fe(CN)_6^{3-/4-}$ from accessing the electrode surface for efficient electron transfer, and a large faradaic impedance response of $Fe(CN)_6^{3-/4-}$ was obtained. Thus, the TPF_{DNA} can represent a "Close" state of the DNA nanostructure. When the TPF_{DNA} modified electrode was further incubated in a solution containing cocaine, the cocaine aptamer P5 was released from the TPF_{DNA} nanostructure and made allosteric changes to bind cocaine, resulting in the "Open" DNA nanostructure. As a result, the TPF_{DNA} nanostructure changed to an Equilateral Triangle DNA nanostructure (defined as ET_{DNA}), resulting in an efficient electron transfer and a small Faradaic impedance response of $Fe(CN)_6^{3-/4-}$. It is worth to mention that the TPF_{DNA} nanostructure can be easily regenerated by placing the ET_{DNA} in cocaine aptamer P5 solution.

2. Experimental

2.1. Reagents and apparatus

All oligonucleotides are synthesized by Sangon Biotech. Co., Ltd. (Shanghai, China). Their sequences are listed in Supplementary information of Table S1. Cocaine, ethylenediaminetetraacetic acid (EDTA), benzoylecgonine (BE), ecgonine methyl ester (EME) and dithiothreitol (DTT) were purchased from Sigma-Aldrich (St. Louis, MO). The synthetic cocaine sample solution was obtained by dissolving cocaine into a 0.9% saline solution. All other chemicals used in this work were of analytical grade. All oligonucleotides were dissolved with 10.0 mM TE buffer (10.0 mM Tris, 1.0 mM EDTA, pH 7.4) into stock solutions and stored at −20 °C. They were diluted with 10.0 mM TE buffer solution to suitable concentrations prior to use. Thiol-modified probes were treated with 0.05 M DTT at room temperature overnight in dark to reduce the S–S bonds prior to use.

The buffer for TPF_{DNA} assembly was 20.0 mM TE (pH 8.0), 50.0 mM $MgCl_2$ and 0.5 M NaCl. The DNA immobilization buffer was 10.0 mM TE (pH 7.4) containing 0.5 M NaCl. The washing buffer was 10.0 mM PB buffer containing 0.1 M NaCl (pH 7.4). Diluent was 0.1 M PBS (pH 7.2). All solutions were prepared with ultrapure water (> 18 MΩ cm) obtained from a Millipore Milli-Q water purification system.

Transmission electron microscopic (TEM) images were acquired with a JEOL JEM-3010 high-resolution transmission electron microscope using an accelerating voltage of 200 kV. Electrochemical experiments were performed with a CHI 660D Electrochemical Workstation (CH Instruments, Shanghai, China). A three-electrode electrochemical cell was used. Au electrode (⌀=2.0 mm, CH Instruments, Shanghai, China) was used as the working electrode. Platinum wire and saturated calomel electrode (SCE) were used as counter and reference electrodes, respectively.

2.2. Formation of TPF_{DNA} and its assembling on Au electrode

The mixture of five oligonucleotides (P1, P2, P3, P4 and P5) in equimolar quantities in TM buffer (20.0 mM TE, 50 mM $MgCl_2$ and 0.5 M NaCl, pH 8.0), was heated to 95 °C for 2 min and then cooled to 4 °C in 30 s.

The Au electrodes were first polished with aqueous slurries of 0.3 μm and 0.05 μm α-Al_2O_3 powders on a polishing microcloth. Then, the Au electrodes were cleaned in "piranha" solution consisting of a 3:1 ratio of H_2SO_4 and H_2O_2 (caution: this mixture reacts violently with organic materials and must be handled with extreme care), then thoroughly washed with ethanol and ultrapure H_2O, and dried under nitrogen. The obtained clean Au electrodes were then immersed in different concentrations of TPF_{DNA} solutions and incubated for different times (from 0.5 to 10 h) in dark at 4 °C. Following the incubation, the electrodes were rinsed with washing buffer. Thus, the capture TPF_{DNA} modified Au electrodes were used for the following experiment.

2.3. Cocaine assays

The obtained TPF_{DNA} modified Au electrode was transferred to a different concentration of cocaine solution and incubated for 30 min. Then, the electrode was extensively rinsed and subjected to electrochemical measurements. Faradaic impedance spectra (FIS) were performed in 1.0 mM $Fe(CN)_6^{3-/4-}$ (1:1) containing 0.1 M NaCl. The impedance measurements were recorded at a bias potential of +179 mV (vs. SCE) within the frequency range from 10 mHz to 10 kHz.

The sensor was regenerated by soaking the electrode in 5.0 μM P5 solution for 3 h at room temperature to ensure the entire ET_{DNA} nanostructure changed to TPF_{DNA}.

3. Results and discussion

3.1. Feasibility study

To determine TPF_{DNA} formation after annealing, high-resolution TEM was performed. As shown in Fig. S1 of Supplementary information, equilateral triangle shape of DNA with an edge length of ~6.0 nm was observed. As expected, the high-resolution TEM of TPF_{DNA} shows a triangular pyramid frustum shape with the edge length and height of ~6.0 nm. These values are almost consistent with the expected length of DNA in Scheme 1, assuming 0.34 nm per base pair (Ke et al., 2012). The above results suggest that tiling and edge-to-edge connections of DNA sequences could be a powerful method to form the 3D DNA nanostructure. The successful assembling of TPF_{DNA} on Au electrode surface was also confirmed by AFM analysis (Fig. S2 in Supplementary information), and the results fit well with the theoretical size value and high-resolution TEM result of the TPF_{DNA}.

Fig. 1 shows the cyclic voltammograms (CVs) and FIS of the TPF_{DNA} modified Au electrode before and after incubation with cocaine. For comparison, CV and FIS of bare Au electrode were also presented. For bare Au electrode, a pair of well-defined and reversible redox peak with the reduction and oxidation peak potentials at 0.144 V and 0.215 V (vs. SCE) was observed (Fig. 1A, curve a). After assembling TPF_{DNA} on Au electrode, the redox peaks became absolutely irreversible with the reduction and oxidation peak potentials at −0.109 V and 0.418 V (vs. SCE), respectively, accompanied with the obvious decrease of peak currents (Fig. 1A, curve b). When the TPF_{DNA} modified electrode was further incubated in cocaine solution, the redox peaks of the modified electrode became a little irreversible with the reduction and oxidation peak potentials at 0.101 V and 0.248 V (vs. SCE), respectively, accompanied with the increase of peak currents (Fig. 1A, curve c). Based on the Laviron theory (Laviron, 1979), the electron transfer rate constant (k_s) of $Fe(CN)_6^{3-/4-}$ at the TPF_{DNA} modified Au electrodes before and after interaction with cocaine was calculated to be $0.0094 \pm 0.0008\ s^{-1}$ and $0.653 \pm 0.052\ s^{-1}$, respectively. This revealed that the k_s value for the TPF_{DNA} modified Au electrodes was approximately 70 times lower than that was interacted with cocaine. Thus, FIS can be used as an effective method for probing the features of interfacial electron-transfer resistance during the sensing process. Fig. 1B shows the FIS (Nyquist plots) at bare Au (curve a) and TPF_{DNA} modified Au electrodes before (curve b) and after (curve c) the electrode treatment with cocaine. By increasing cocaine concentration, the interfacial electron resistance decreased dramatically, coinciding with the CV results. Thus, cocaine addition would result in the activation of the DNA nanostructure from "Close" to "Open" and accordingly generate the interfacial electron resistance (R_{et}) corresponding to the status of the DNA nanostructure. Unlike those previous strategies for signal "On/Off" and reversible sensing, the stability and regeneration ability for multi-regeneration performance were not satisfied, due to the instability of the redox labels or single thiolated probes (Yang and Lai, 2012). The proposed 3D DNA nanostructure system was stable enough to operate for several cycles without significant decay, and multiple resets upon washing the electrode and addition of new chemical inputs were possible (Fig. S3 in Supplementary information).

3.2. Optimization

In order to obtain satisfied assay result, some factors are investigated in detail. It has been proved that the conformational effects are sensitively dependent on the surface densities of the assembled sensing units. The surface density of TPF_{DNA} on the Au electrode is a crucial parameter contributing to signal gain, which can be controlled by varying the probe concentration during sensor fabrication. To optimize the signal gain, the performance of the sensors fabricated with different concentrations of TPF_{DNA} (0.1–5.0 μM) was studied under the same concentration of 100 nM target cocaine. The change of ΔR_{et} ($\Delta R_{et} = R_{et}^0 - R_{et}$) is used to characterize the change of electrode surface. It was clearly observed that the ΔR_{et} increased with the increase of surface density when the concentration of TPF_{DNA} was 1.0 μM. The surface density of the TPF_{DNA} surface was calculated to be 3.2×10^{12} probe/cm^2. Hence, 1.0 μM TPF_{DNA} is chosen as the optimized concentration for the following experiment. Next, the assembling time of TPF_{DNA} on Au electrode surface and incubation time of TPF_{DNA} with cocaine were checked. It was found that the ΔR_{et} signals initially increased rapidly over time for assembling and incubation, then became saturated until 30 min and 20 min. Thus, 30 min assembling time and 20 min incubation time were used in the standard procedures.

3.3. Cocaine detection

Under the optimized condition, the relationship between R_{et} value and the concentrations of synthetic cocaine sample is studied (Fig. 2A). $\Delta R/R_{et}^0$ (defined as $(R_{et}^0 - R_{et})/R_{et}^0$) is used for evaluating the concentrations of target cocaine. As shown in Fig. 2B, there is a linearity relationship between $\Delta R/R_{et}^0$ and the function of the logarithm of the concentration of cocaine over a wide concentration range from 1.0 nM to 2.0 μM ($R^2 = 0.993$). The linear response obtained with the sensor covers the lethal blood levels for a range of 0.33–69.0 nM cocaine (Mittleman and Wetli, 1984), indicating that the sensor could be possibly used in the analysis of real samples. The limit of detection (LOD) of this method was calculated following IUPAC recommendations ($3S_b/b$, where S_b is the standard deviation ($n = 11$) of the blanks, and b is the slope value of the respective calibration graph) at a concentration level of 0.21 nM. Comparing with the results reported by some literatures (Table S2 in Supplementary information), this value is superior to most available cocaine aptasensors. Moreover, the sensitivity for cocaine detection calculated from the slope of the respective calibration graph was 26.2 kΩ/log([cocaine]/(nM)), which is over six-fold enhancement over an impedimetric biosensor based on supramolecular aptamer fragments/target complex (Zhang et al., 2012), indicating the high sensitivity of the proposed sensing system.

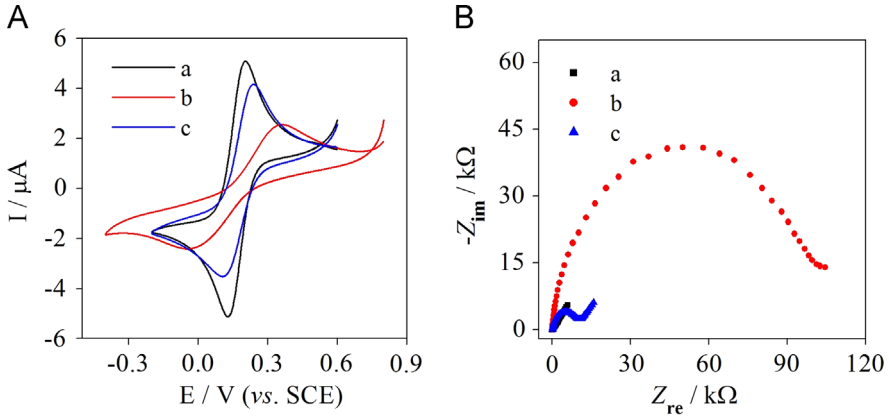

Fig. 1. CVs (A) and FISs (B) of the (a) bare and (b) and (c) DNA nanostructure modified electrodes in a 1.0 mM $Fe(CN)_6^{3-/4-}$ (containing 0.1 M NaCl) solution. Here, (b) was the "Close" state of TPF_{DNA} and (c) was the TPF_{DNA} modified electrode after interaction with cocaine. Scan rate: 50 mV s^{-1}. Applied potential: +0.179 V (vs. SCE). Frequency range: 10 mHz to 10 kHz. Amplitude: 5 mV.

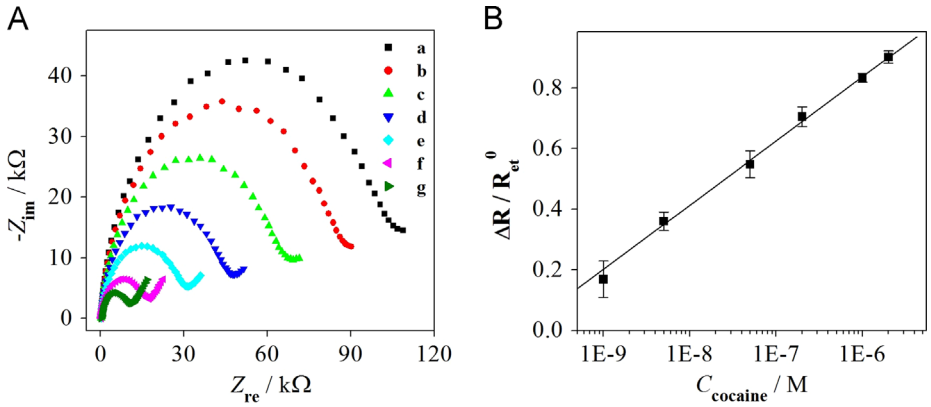

Fig. 2. (A) FIS curves of the "Close" state of TPF_{DNA} modified Au electrodes in a 1.0 mM $Fe(CN)_6^{3-/4-}$ (containing 0.1 M NaCl) solution corresponding to different concentration of cocaine. (a) 0, (b) 1.0 nM, (c) 5.0 nM, (d) 50.0 nM, (e) 0.2 μM, (f) 1.0 μM and (g) 2.0 μM. (B) The corresponding calibration plot of $\Delta R/R_{et}^0$ vs. different concentrations of cocaine.

3.4. Detection in real-life samples

To assess the 3D DNA based sensor's ability to detect small molecules in complex, we tested the ability to detect cocaine in the presence of other contaminants and in biological fluids. Cocaine metabolites, BE and EME were chosen as negative controls. The results were shown in Fig. S4(A) of Supplementary information. There were only weak $\Delta R/R_{et}^0$ changes after addition of BE and EME (each 1.0 μM) into the TPF_{DNA} sensing system, indicating that the sensing platform has excellent selectivity.

The sensor was used to detect cocaine in 20% and 50% human serum (Fig. S4(B)) diluted with buffer in comparison with those in blank buffer. Studies showed that the R_{et} signal decreased by 84.5% and 82.6%, respectively, when 1.0 μM of cocaine was added in 20% and 50% human serum. Moreover, the detection limits were close to those obtained in blank buffer, suggesting that the other components of the serum did not interfere significantly with sensor performance. Analysis of cocaine in 1% and 10% human urine samples was also conducted. As shown in Fig. S4, the R_{et} signal decreased by 85.0% and 84.2%, respectively. Thus, the successful detection of cocaine in serum and urine as demonstrated here may be straightforward when testing for cocaine clinically.

4. Conclusions

In summary, an ultrasensitive electrochemical cocaine biosensor based on the structure conversion of 3D DNA nanostructure was presented. The prepared biosensor exhibited stable, regenerable, and sensitive functions for cocaine determination. Additionally, we may except that coupling the 3D DNA nanostructure conversion with unique signaling and/or structural features, the performances of the biosensor will be further improved. The principle of the 3D DNA nanostructure conversion strategy could potentially be used to construct nanoswitches, nanoreactors, and biosensors, even pointing to future applications in clinical settings for biological fluids.

Acknowledgments

The authors gratefully acknowledge the financial supports by the NSFC (No. 21105080), the SRFDP (No. 20126101120023), the NSF of Shaanxi Province (Nos. 2012JQ2010, 2012JM2013, and 2013KJXX-25), the Scientific Research Foundation of Shaanxi Provincial Key Laboratory (11JS080 and 12JS087) and the Scientific Research Program of Shaanxi Provincial Education Department (No. 12JK0576).

Appendix A. Supporting information

Supplementary data associated with this article can be found in the online version at http://dx.doi.org/10.1016/j.bios.2013.07.053.

References

Carrasquilla, C., Lau, P.S., Li, Y.F., Brennan, J.D., 2012. Journal of the American Chemical Society 134 (26), 10998–11005.
Douglas, S.M., Dietz, H., Liedl, T., Hogberg, B., Graf, F., Shih, W.M., 2009. Nature 459 (7425), 414–418.
Jiang, B.Y., Wang, M., Chen, Y., Xie, J.Q., Xiang, Y., 2012. Biosensors and Bioelectronics 32 (1), 305–308.
Kang, D., Vallée-Bélisle, A., Porchetta, A., Plaxco, K.W., Ricci, F., 2012. Angewandte Chemie International Edition 51 (27), 6717–6721.
Ke, Y.G., Voigt, N.V., Gothelf, K.V., Shih, W.M., 2012. Journal of the American Chemical Society 134 (3), 1770–1774.
Laviron, E., 1979. Journal of Electroanalytical Chemistry 100 (1–2), 263–270.
Li, Z., Wei, B., Nangreave, J., Lin, C.X., Liu, Y., Mi, Y.L., Yan, H., 2009. Journal of the American Chemical Society 131 (36), 13093–13098.
Liu, J.W., Cao, Z.H., Lu, Y., 2009. Chemical Reviews 109 (5), 1948–1998.
Mittleman, R.E., Wetli, C.V., 1984. Journal of the American Medical Association 252 (14), 1889–1893.
Pei, H., Liang, L., Yao, G.B., Li, J., Huang, Q., Fan, C.H., 2012. Angewandte Chemie International Edition 124 (36), 9154–9158.
Pei, H., Lu, N., Wen, Y.L., Song, S.P., Liu, Y., Yan, H., Fan, C.H., 2010. Advanced Materials 22 (42), 4754–4758.
Soloveichik, D., Seelig, G., Winfree, E., 2010. Proceedings of the National Academy of Sciences of the United States of America 107 (12), 5393–5398.
Surana, S., Bhat, J.M., Koushika, S.P., Krishnan, Y., 2011. Nature Communications 2, 340.
Vallée-Bélisle, A., Bonham, A.J., Reich, N.O., Ricci, F., Plaxco, K.W., 2011. Journal of the American Chemical Society 133 (35), 13836–13839.
Wang, F.A., Elbaz, J., Orbach, R., Magen, N., Willner, I., 2011a. Journal of the American Chemical Society 133 (43), 17149–17151.
Wang, Z.G., Elbaz, J., Willner, I., 2011b. Nano Letters 11 (1), 304–309.
Wen, Y.L., Pei, H., Wan, Y., Su, Y., Huang, Q., Song, S.P., Fan, C.H., 2011. Analytical Chemistry 83 (19), 7418–7423.
Willner, I., Zayats, M., 2007. Angewandte Chemie International Edition 46 (34), 6408–6418.
Xiang, Y., Qian, X.Q., Zhang, Y.Y., Chai, Y.Q., Yuan, R., 2011. Chemical Communications 47 (7), 2080–2082.
Yang, W.W., Lai, R.Y., 2012. Chemical Communications 48 (69), 8703–8705.
Yeung, M.C.L., Wong, K.M.C., Tsang, Y.K.T., Yam, V.W.W., 2010. Analyst 46 (41), 7709–7711.
Zhang, D.W., Zhang, F.T., Cui, Y.R., Deng, Q.P., Krause, S., Zhou, Y.L., Zhang, X.X., 2012. Talanta 92, 65–71.
Zhou, M., Du, Y., Chen, C.G., Wen, D., Dong, S.J., Wang, E.K., 2010. Journal of the American Chemical Society 132 (7), 2172–2174.